Sean D. Mooney[1,2]
Peter A. Kollman[2]*
Teri E. Klein[1]
[1] *Stanford Medical Informatics, 251 Campus Drive, MSOB X-215, Stanford University, Stanford, CA 94305-5479*

[2] *Department of Pharmaceutical Chemistry, University of California San Francisco, San Francisco, CA 94143-0446*

Received 28 August 2001; accepted 11 December 2001

Conformational Preferences of Substituted Prolines in the Collagen Triple Helix

Abstract: *Researchers have recently questioned the role hydroxylated prolines play in stabilizing the collagen triple helix. To address these issues, we have developed new molecular mechanics parameters for the simulation of peptides containing 4(R)-fluoroproline (Flp), 4(R)-hydroxyproline (Hyp), and 4(R)-aminoproline (Amp). Simulations of peptides based on these parameters can be used to determine the components that stabilize hydroxyproline over proline in the triple helix. The dihedrals F–C–C–N, O–C–C–N, and N–C–C–N were built using a N-β-ethyl amide model. One nanosecond simulations were performed on the trimers $[(Pro–Pro–Gly)_{10}]_3$, $[(Pro–Hyp–Gly)_{10}]_3$, $[(Pro–Amp–Gly)_{10}]_3$, $[(Pro–Amp^{1+}–Gly)_{10}]_3$, and $[(Pro–Flp–Gly)_{10}]_3$ in explicit solvent. The results of our simulations suggest that pyrrolidine ring conformation is mediated by the strength of the gauche effect and classical electrostatic interactions.* © 2002 Wiley Periodicals, Inc. Biopolymers 64: 63–71, 2002

Keywords: *molecular dynamics; collagen-like peptides; triple-helix; fluoroproline; hydroxyproline*

INTRODUCTION

Collagen is the most abundant protein in mammals and is characterized by the presence of a triple helix. The triple helix contains a repeating X–Y–Gly amino acid triplet motif. Proline is the most abundant residue in the triple helix and Y-position prolines are often posttranslationally hydroxylated. The collagen triple helix exhibits unusual stability, in part, due to the conformational properties of proline residues. The components that stabilize the triple helix are an area of active research. Recent results suggest that the preference of proline residues in the X and Y positions is not entirely due to the presence of a tertiary amine.[1]

Hydroxyprolines (Hyp) in the Y position of collagen's repeating X–Y–Gly triplet further stabilize the

Correspondence to: Teri E. Klein; email: teri.klein@smi.stanford.edu
Contract grant sponsor: NIH
Contract grant sponsor: AR47720-01
*Peter Andrew Kollman passed away on May 25, 2001
Biopolymers, Vol. 64, 63–71 (2002)

folded state by approximately 0.2 kcal/(mol triplet).[2–4] Historically, this increased stability was proposed to be mediated by hydrogen bonding of the pyrrolidine hydroxyl with solvent.[5–7] Unlike hydroxyproline, fluoroproline (Flp) cannot hydrogen bond well with solvent, yet Pro–Flp–Gly was shown to be the most stable triplet known.[8] Researchers have also shown that aminoproline with an electron withdrawing effect and solvent hydrogen-bonding potential stabilizes the triple helix to a larger degree than hydroxyproline.[9] The stabilizing effect of hydroxyproline over proline is stereoselective and position dependent in that only hydroxyproline residues with R stereochemistry[10,11] in the Y position are stabilizing.[3,12] This stereoselectivity favoring the R stereoisomer over S is proposed to arise from the overlap of an electron pair with the antibonding σ^* of an adjacent polar bond (C–X, where X—N or O).[10]

Proline residues can adopt two ring pucker conformations, Cγ-*exo* and Cγ-*endo* (Figure 1). The Cγ-*exo* conformation places the Cγ carbon puckered away from the Cα—C backbone bond. Substituted prolines with R stereochemistry adopt two conformations for the N–C–C–X torsion angle. When the pyrrolidine ring is Cγ-*endo*, the substituted N–C–C–X dihedral angle adopts nearly the anti conformation (Figure 1b). The Cγ-*exo* conformation places the N and X substituent in the gauche conformation[13] (Figure 1c). The N–C–C–F dihedral has been shown to have an especially strong gauche effect and shows a nearly 1.8 kcal/mol *gauche* preference in model compounds.[14] It has recently been proposed that this conformation of hydroxyproline stabilizes the folded collagen trimer by adopting a conformation preferred by Y-position in the triple helix.[15] This theory would support both the stereo-selectivity of the Y position and the observation that hydroxyprolines in the X position destabilize the triple helix.

To analyze pyrrolidine ring conformational preferences, we have built models for idealized collagen-like peptides with proline, hydroxyproline, fluoroproline, and both the charged and neutral aminoproline residues in the Y position. These models can be used in a manner similar to those previously published to determine dihedral angle parameters for molecular mechanics force fields.[16] Using the new dihedral parameters, we have performed one nanosecond simulations on the folded trimers, $[(\text{Pro–Pro–Gly})_{10}]_3$, $[(\text{Pro–Hyp–Gly})_{10}]_3$, $[(\text{Pro–Amp–Gly})_{10}]_3$, $[(\text{Pro–Amp}^{1+}\text{–Gly})_{10}]_3$, and $[(\text{Pro–Flp–Gly})_{10}]_3$ in explicit solvent. We can use these models to describe how electron withdrawing effects alter the conformation of substituted pyrrolidine rings and the structure of solvent around the triple helix. Our results predict that

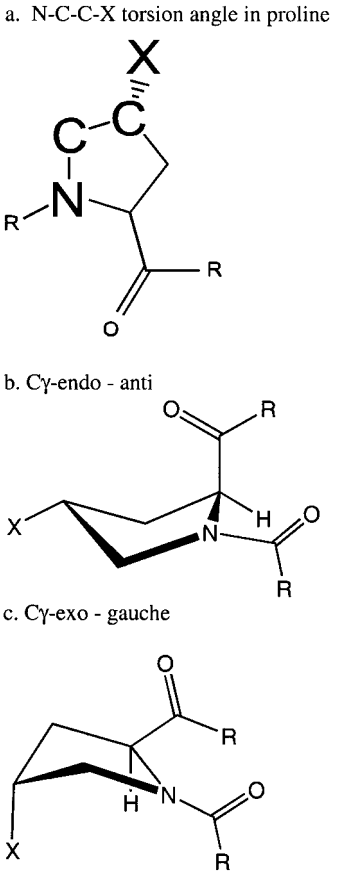

FIGURE 1 Pyrrolidine ring conformation. Illustration of the conformations adopted by pyrrolidine ring. (a) N–C–C–X torsion angle. (b) Cγ-*exo* conformation of an X-substituted proline residue. (c) The Cγ-*endo* conformation illustrated in a manner similar to (b).

Cγ-*exo* preference of substituted proline residues is shifted by the magnitude of gauche preference of the N–C–C–X dihedral and electrostatic interactions of the polar substituent with other polar groups of the solute.

METHODS

Parameters

We have developed new molecular mechanics parameters to investigate recent evidence[3] suggesting that a *gauche* effect occurs in 4(R)-substituted prolines. The developed parameters are the F–C–C–N, O–C–C–N, N–C–C–N, and N^{1+}–C–C–N torsion angles and point charges for 4(R)-L-fluoroproline, 4(R)-L-aminoproline, and 4(R)-L-aminoproline^{1+}. Point charges for 4(R)-L-hydroxyproline were developed previously.[17]

Point charges for 4(R)-L-fluoroproline and the neutral and charged forms of 4(R)-L-aminoproline were developed using the published two-stage RESP fitting process.[18] Four

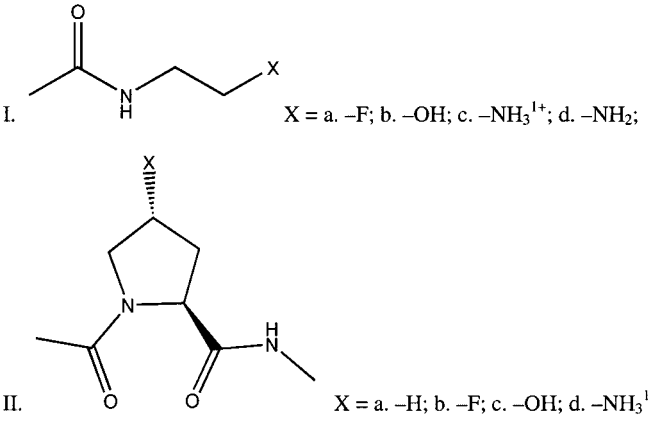

FIGURE 2 Parameterization structure. Structural models used in parameterization of the proline ring preferences. Structure I is an N-β-ethyl amide model developed by O'Hagan et al.[14] Structure II is the model used to determine single residue ring conformational preferences.

conformations were used for the fitting corresponding to the four most common conformations of prolines in protein structures.[19] The conformations represent the two ring puckers (α,β) and the two ω torsion angles (*cis*, *trans*).[20] Geometry optimization was performed on each structure using the 6-31G* basis set and a Hartree–Fock level of theory. The electrostatic potential was determined for each structure using MP2 level of theory and the 6-31G* basis set. All quantum mechanical calculations were performed with Gaussian98.[21] The charges were then determined using the RESP program following the protocols published for proline and hydroxyproline.

The F–C–C–N torsion angle was recently shown to have an unusually strong *gauche* effect mediated by the strong F and N electron withdrawing groups.[14] These dihedral angle parameters were developed using the N-β-ethyl amide model developed by O'Hagan et al.[14] (Figure 2, structure I). For I.a, I.b, I.c, I.d, and I.e, the *anti* and *gauche* conformations were optimized at the Hartree–Fock level of theory using the 6-31G* basis set. Next, single point energies were determined using MP2 level of theory and the 6-31G* basis set. The electrostatic potential for each conformation was used to develop a charge model for molecular mechanics.

After RESP determination of AMBER point charges, each conformation was minimized for 10,000 steps. AMBER energies were determined and a V2 dihedral was added to make the AMBER energies equivalent to the ab initio model. These parameters were then used to simulate the appropriate substituted pyrrolidine ring.

Simulations

For the folded trimer simulations, the initial structures were modeled from pdb:1cgd[22] using a protocol similar to that previously published.[17] One nanosecond simulations were performed for $[(Pro–Pro–Gly)_{10}]_3$, $[(Pro–Hyp–Gly)_{10}]_3$, $[(Pro–Flp–Gly)_{10}]_3$, $[(Pro–Amp–Gly)_{10}]_3$, $[(Pro–Amp^{1+}–Gly)_{10}]_3$, $[(Pro–Pro–Gly)_4(Pro–Hyp–Gly)(Pro–Pro–Gl)_5]_3$, $[(Pro–Pro–Gly)_4(Pro–Flp–Gly)(Pro–Pro–Gly)_5]_3$, $[(Pro–Pro–Gly)_4(Pro–Amp–Gly)(Pro–Pro–Gly)_5]_3$, and $[(Pro–Pro–Gly)_4(Pro–Amp^{1+}–ly)(Pro–Pro–Gly)_5]_3$ using the AMBER 6.0 molecular simulation package. Each simulation was carried out using periodic boundary conditions in explicit solvent with 12.0 Å of solvent from the solute to the edge of the box. Production dynamics was then performed at 300 K.

Structural Analysis

For each simulation, the *gauche* effect was calculated by determining the average ring pucker for each position along the chain. The ring pucker state was determined using the Ptraj program in the AMBER package. For the folded trimers, each Y-position amino acid was monitored once every 10 frames (2 ps) for each frame after 120 ps excluding the first and last two triplets of each chain. The ring pucker state was then determined by monitoring the conformation of the ring. Each pucker was assigned to be either Cγ-*exo* or Cγ-*endo*. In the folded simulations saturated with substituted prolines, the ring pucker state was averaged and reported for each of the monitored 18 Y positions as the fraction of the time that the ring is Cγ-*exo* along with the standard deviation between the positions. The main-chain dihedrals of the triple helix was monitored throughout each of folded trimer simulations.

Simulations were also available to compare the differences in the ring pucker conformation with and without the added parameters to model the γ *gauche* effect for the substituted Pro–Flp–Gly and Pro–Hyp–Gly trimers. These initial simulations are similar to those reported here except they do not contain the new F–C–C–N and O–C–C–N dihedral parameters and slightly less solvent molecules (8.0 Å radius to edge of box vs 12.0 Å). These results are reported to illustrate the effect of the *gauche* effect on folded triple helices.

To assess whether observed solvent structural patterns around the triple helix is composed of fixed solvent mole-

Table I Parameterization Energies[a] of Substituted N-β-Ethyl Amides (I.a–d)

Structure Dihedral	MP2[b]	AMBER[c]	AMBER Params[d]
I.a F–C–C–N			
gauche	−385.910585 au	−27.9872	−27.7767
anti	−385.907879 au	−27.1757	−25.9972
Difference	−1.697 kcal/mol	−0.8115	−1.7795
I.b. O–C–C–N			
gauche	−361.920163 au	−39.5638	−39.371
anti	−361.916517 au	−37.6242	−37.0934
Difference	−2.286 kcal/mol	−1.9396	−2.2857
I.c N–C–C–N			
gauche	−342.4663614 au	−15.2566	−14.7884
anti	−342.4298653 au	−0.6745	8.0672
Difference	−22.883 kcal/mol	−14.5821	−22.8556
I.d N–C–C–N			
gauche	−342.0807528 au	−50.1153	−49.7764
anti	−342.0765046 au	−48.2528	−47.1119
Difference	−2.664 kcal/mol	−1.8625	−2.6645

[a] Values in kcal/mol except absolute MP2 energies. Differences in ab initio and semiempirical conformational energies of the N-β-ethyl amide models illustrated in Figure 2.
[b] MP2 energies determined using Gaussian98 and the 6-31G* basis set.
[c] AMBER energies determined using the Parm94 force field.
[d] AMBER energies determined using the Parm94 force field and the parameters shown in Table II.

cules or a dynamic shell, the length of time each solvent/solute hydrogen bond exists was measured for hydroxyproline containing triplets. This data was histogramed and the average length of a hydrogen bond was calculated. To analyze differences between peptides, the average number of solvent molecule contacts per residue and per atom was calculated for each simulation.

RESULTS

Parameters

Geometry optimization on the substituted N-β-ethyl amides was completely unrestrained except for the *anti* conformation of I.d, which was held at 180°. Single point energies are shown in Table I. The quantum mechanical model energies were then used to parameterize the molecular mechanics dihedrals. The *anti*/*gauche* MP2 energy difference for I.a was −1.697 kcal/mol, which is in good agreement with previous studies.[14] The unmodified molecular mechanics energy showed a slight *gauche* preference at − 0.81 kcal/mol. A V2 dihedral parameter of 0.569 was added to the AMBER force field to model the *gauche* effect and gives a *gauche* preference of −1.78 kcal/mol, the published energy. Interestingly, for I.b, the ab initio model predicted the gauche preference to be −2.286 kcal/mol. The unmodified molecular mechanics energy difference is −1.94 kcal/mol. A V2 dihedral parameter of 0.269 was added to model the *gauche* effect. However, the AMBER dihedral term is lower in magnitude, suggesting the enhanced *gauche* preference in this case is due to classical electrostatics and not quantum mechanical effects. Parameterization for the charged amino substituted compound (I.c) was performed in a similar manner. Because of large electrostatic differences, a V2 term of 4.5 was added to reproduce the ab initio result in the molecular mechanics model. The full torsional parameters are summarized in Table II.

Simulations

Four 1-ns simulations were performed for each of the folded peptides with explicit solvent. Each simulation contained 90 residues and approximately 5500 TIP3P waters. Aminoproline triplets were simulated in acidic conditions, with one chloride atom added per triplet to neutralize the simulation. When compared to AMBER simulations with default parameters, the expected increase in Cγ-*exo* ring preference is observed (Table III).

To compare whether these observations depend on the presence of neighboring substituted prolines in the Y position, simulations were then performed with a single substituted proline in the center of each chain. All other Y positions are proline. In this case, the

Table II Dihedral Parameters[a,b]

	PK	PN[c]
H1–CT–CT–N	0.156	1
OH–CT–CT–N	0.269	2
	0.156	1
F–CT–CT–N	0.569	2
	0.156	1
N3–CT–CT–N[d]	4.50	2
	0.156	1
N3–CT–CT–N[e]	0.572	2
	0.156	1

[a] $E_{\text{dihedrals}}$ = (PK/IDIVF) * [1 + cos(PN * φ − PHASE)].
[b] IDIVF = 1.0 and PHASE = 0.0 for all parameters.
[c] Parameters where PN = 1 are standard in the Amber Parm94 force field. To develop additional parameters, terms with a PN = 2 were added.
[d] Amine has +1 charge.
[e] Amine is neutral.

results are similar to that of the folded case, implying that the increased preference in Cγ-*exo* pyrrolidine ring conformation is independent of the other positions. Differences in conformation are seen by position along the length of the triple helix as well. Figure 3 illustrates this by showing how each of the proline residue's conformation differs by position. As is suggested in the figure, neutral residues with hydrogen-bonding potential differ more than the others, perhaps due to their need to hydrogen bond with solvent. Table IV illustrates the preferred dihedral angles in position of the folded trimer simulations. As was shown from crystallographic[15,23] and NMR studies[24] of the Pro–Pro–Gly and Pro–Hyp–Gly trimer, our simulations predict a Y-position ϕ conformation of -58.5 ± 0.7 and a X-position ϕ conformation of -70.1 ± 0.8. These results support the theory that hydroxyproline prefers the backbone conformation in the Y position.[15]

The average length of time each solvent/solute hydrogen bond exists is 0.50 ± 1.02 (4.5 ± 9.18 ps). A histogram showing the time distribution of hydrogen bonds is shown in Figure 4. As can be seen, the majority of hydrogen bonds are present less than 5% (45 ps) of the time and none are present for greater than 15% (135 ps) of the time. The few that are present greater than 10% of the time are observed in a configuration where solvent bridging interactions are feasible with solvent bridging. The longest hydrogen bond present is a 135-ps interaction between the amide nitrogen of glycine 15 chain B and a solvent molecule. That solvent molecule is also seen hydrogen bonding with the hydroxyl group of several hydroxyproline residues but none of those interactions last longer than 14.4 ps. This data is inconsistent with the theory that solvent molecules are binding specifically to Pro–Hyp–Gly trimer.

Table V and Figure 5 show differences in solvent structure per atom for each of the residues. We find that solvent structure correlates with molecular weight of the Y-position residue. Interestingly, fluoroproline shows slightly less solvent molecules than all the other Y-position residues simulated.

DISCUSSION

We have found that ab initio calculations predict a strong *gauche* effect for the F–C–C–N torsion angle. Our results show that the O–C–C–N torsion angle exhibits a stronger *gauche* preference, but a weaker quantum mechanical *gauche* effect in our model system. The finding that AMBER simulations without new parameters show slight *gauche* preferences suggests that there is a classical electrostatic component to these preferences. These interactions are likely between the polar substituent and other polar groups in the N-β-ethyl amide model. When these results are applied to substituted pyrrolidine rings,

Table III Preferred Pucker Conformation (in Percent Cγ-*exo*)[a]

	Pro–Pro–Gly[c]	Pro–Hyp–Gly	Pro–Flp–Gly	Pro–Amp^{1+}–Gly	Pro–Amp–Gly
Default parameters[b]	61.9 (4.8)	50.4 (9.1)	68.8 (7.7)	N/A	N/A
New dihedral parameters	59.8 (4.3)	62.8 (9.4)	84.8 (4.2)	95.9 (2.1)	45.3 (9.2)
Three residue folded[d]	N/A	54.3 (3.8)	84.0 (7.5)	92.0 (5.2)	31.0 (22.3)

[a] Values are given in percent Cγ-*exo*. Standard deviations from each position are in parentheses.
[b] Simulations with the default parameters were run previously and are unpublished. Conditions are identical with the exception of a distance 2 Å less between the solute and the edge of the water box.
[c] Re-ran as a control and to maintain identical simulation conditions as with other simulations. Solute parameters between simulations are identical.
[d] Simulations of $[(\text{Pro–Pro–Gly})_{10}]_3$ with a single, central Y-position proline residue in each chain (position 14). Standard deviation is from the average of those three positions.

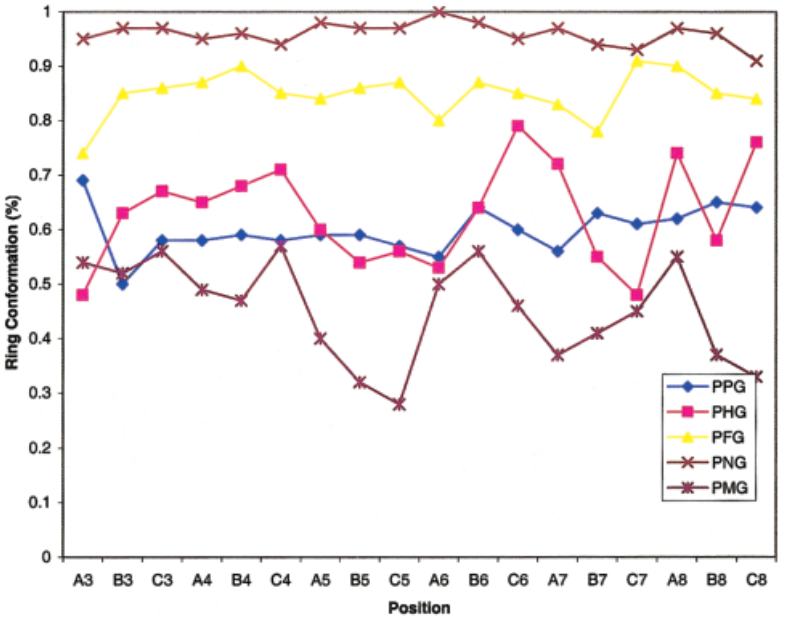

FIGURE 3 Proline ring preferences by position. Conformational preferences by position of the pyrrolidine ring pucker. PPG is $[(Pro–Pro–Gly)_{10}]_3$. PHG is $[(Pro–Hyp–Gly)_{10}]_3$. PFG is $[(Pro–Flp–Gly)_{10}]_3$. PNG is $[(Pro–Amp–Gly)_{10}]_3$. PMG is $[(Pro–Amp^{1+}–Gly)_{10}]_3$. *Y* axis is in percent Cγ-*exo* and *X* axis is the residue number in the form of chain/triplet number (example: A3 is the third triplet in chain A).

we find that the *gauche* effect enhances the preference for the Cγ-*exo* ring conformation. The dihedral parameters developed for hydroxyproline may be relevant for serine and threonine as well, because the bond order and environment are similar to the OG–CB–CA–N dihedral.

In a folded triple helix, the Cγ-*exo* conformation is preferred in proline, hydroxyproline and fluoroproline. Fluoroproline shows a stronger gauche preference over both hydroxyproline and proline. These results support the theory that electron withdrawing effects alter the preferred conformation of substituted proline residues in collagen.[3,10,13]

When the different groups substituents (—H, —OH, —F, $—NH_2$, $—NH_3^{1+}$) are compared, we observe that fluoroproline and the charged aminoproline have the greatest Cγ-*exo* preference, while hydroxyproline and the uncharged amino proline have less Cγ-*exo* preference. This seems to contradict our

Table IV Average Values of Peptide Dihedral Angles[a]

Dihedral	Pro–Pro–Gly	Pro–Hyp–Gly	Pro–Flp–Gly	Pro–Amp^{1+}–Gly	Pro–Amp–Gly	Pro–Hyp–Gly X-Ray[23]	Collagen Ideal[28]
x ϕ	−70.13 (0.8)	−69.69 (1.1)	−69.64 (0.7)	−66.87 (1.6)	−69.60 (0.8)	−75.0	−72.1
X ψ	161.18 (0.5)	163.06 (0.9)	162.23 (0.7)	163.70 (1.2)	162.87 (1.1)	161.4	164.3
X ω	174.18 (0.5)	174.71 (0.7)	173.59 (0.6)	177.4 (1.6)	174.85 (1.0)	177.8	180.0
Y ϕ	−58.51 (0.7)	−58.34 (1.1)	−55.91 (0.7)	−59.33 (1.2)	−60.82 (1.7)	−61.0	−75.0
Y ψ	152.46 (0.7)	153.70 (0.8)	151.83 (0.6)	159.95 (3.7)	153.94 (1.8)	153.3	155.8
Y ω	179.42 (0.7)	179.02 (0.6)	178.55 (0.7)	175.70 (2.1)	179.30 (0.9)	176.7	180.0
G ϕ	−74.60 (0.8)	−75.95 (0.8)	−75.16 (1.1)	−79.15 (6.6)	−76.45 (5.3)	−75.8	−67.6
G ψ	176.11 (0.7)	177.60 (0.8)	178.02 (1.0)	160.36 (4.1)	175.89 (2.5)	179.9	151.4
G ω	177.78 (0.4)	177.24 (0.4)	177.39 (0.5)	176.87 (1.2)	177.74 (1.3)	179.5	180.0

[a] Values are in degrees. Standard deviations are shown in parentheses. Comparison of the measured dihedrals for the folded trimer simulations $[(Pro–Pro–Gly)_{10}]_3$, $[(Pro–Hyp–Gly)_{10}]_3$, $[(Pro–Flp–Gly)_{10}]_3$, $[(Pro–Amp–Gly)_{10}]_3$, $[(Pro–Amp^{1+}–Gly)_{10}]_3$.

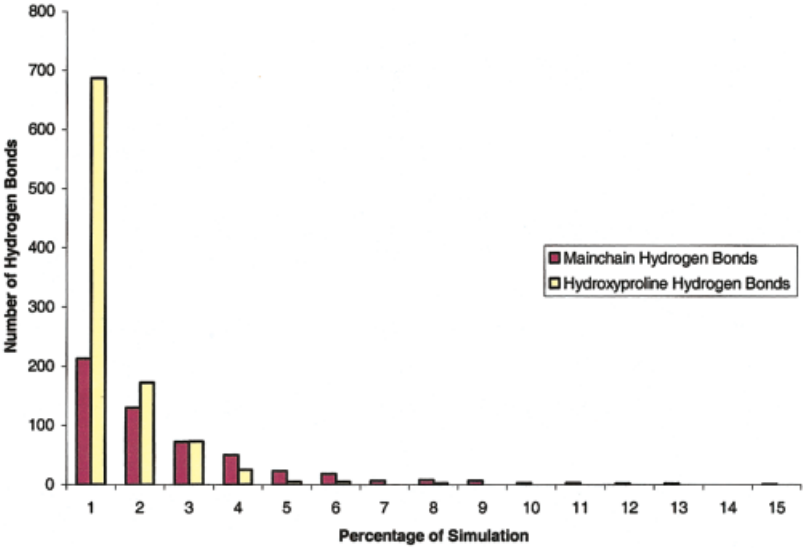

FIGURE 4 Average time of solvent/solute hydrogen bonds for Pro–Hyp–Gly. Number of solvent/solute hydrogen bonds that are present at that percentage of the simulation. The total time of analysis is 900 ps; therefore, each percentage point is equal to 9 ps. The *Y* axis is the number of hydrogen bonds and the *X* axis is the percentage of the simulation that the hydrogen bonds must persist. The graph indicates that solvent molecules generally exchange hydrogen bonds very quickly (faster than 270 ps) around the surface of the triple helix. Main-chain hydrogen bonds are not as common, but exchange less often than hydroxyproline hydrogen bonds. Solvent/solute hydrogen bonds involving the first two and last two triplets were not considered for the analysis.

observation from the N-β-ethyl amide models where the hydroxyl and amine groups show a greater *gauche* preference than fluoroproline (Table I and Table III). We explain these inherent differences caused by moving from a simple N-β-ethyl amide model to a solvated triple helix. It is interesting that both of the uncharged substituents with hydrogen-bonding potential (—OH and —NH_2) exhibit a wider range of observed conformations than any of the others (Figure 3). This may be due to environmental differences, solvent structure differences, or neighboring residues interaction differences.

The importance of solvent molecules is a matter of considerable debate within the collagen community. Research reporting the presence of solvent structure is well documented by many groups.[6,7,15,22,25] Here we predict that this structure can only be composed of solvent/solute hydrogen bonds that are rapidly exchanging with each other. These results are inconsistent with previous models that propose a stabilizing effect of specifically bound solvent molecules. Structural differences do exist, however, between the different residues. Table V and Figure 5 illustrate these differences and show that fluoroproline shows the smallest number of water molecules per Y-position residues and the charged aminoproline shows the largest number of solvent molecules.

Our efforts are now directed at building an energetic model of the enhanced stability of fluoroprolines and in analyzing solvent structure differences in our peptides. We have previously used thermodynamic integration calculations to show how glycine to ala-

Table V Average Solvent Molecules Per Atom Per Frame (R < 4 Å)[a]

	Y = Pro	Flp	Hyp	Amp	Amp1+
Pro	3.40 (.12)	3.26 (.08)	3.42 (.11)	3.56 (.42)	3.75 (.26)
Y	3.68 (.15)	3.59 (.13)	4.07 (.11)	4.52 (.37)	5.12 (.34)
Gly	1.15 (.11)	1.08 (.10)	1.07 (.08)	1.50 (.75)	1.62 (.64)

[a] Standard deviations are shown in parentheses. Calculated using all residues excluding the four terminal triplets in each chain. Averaged over 100 ps of dynamics.

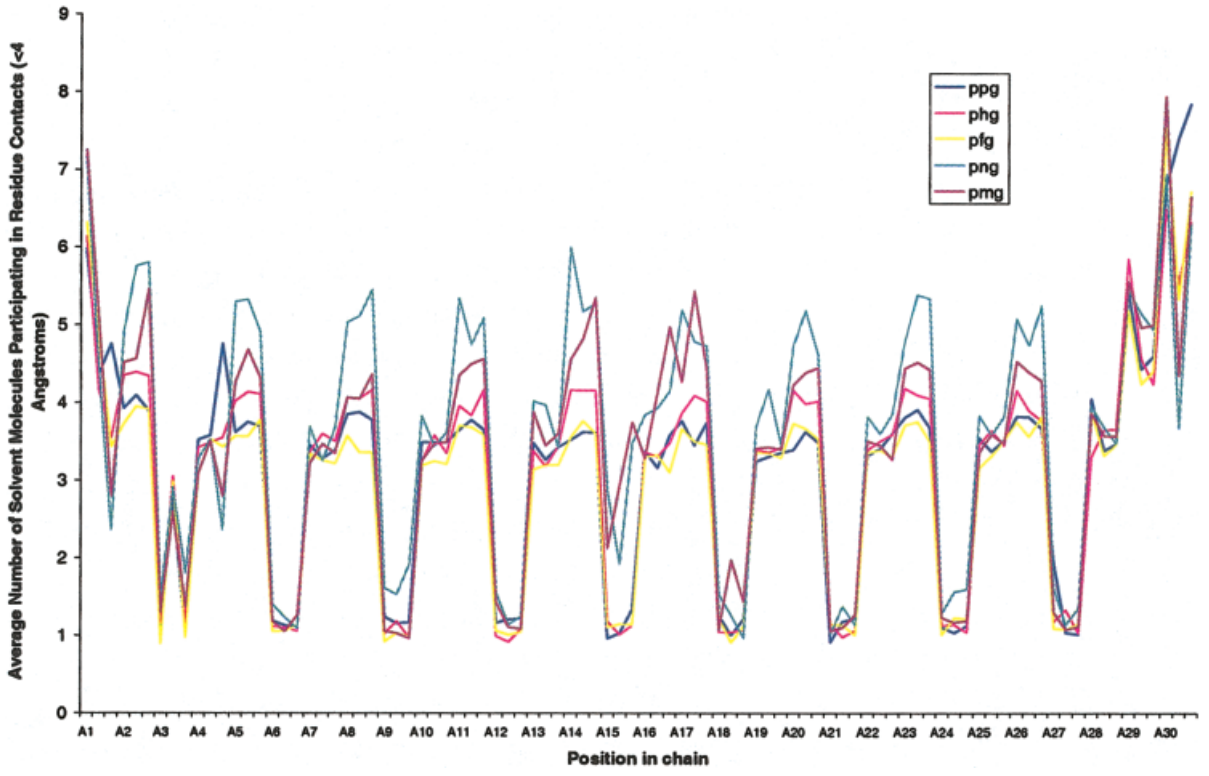

FIGURE 5 Average solvent molecules per atom per frame ($R < 4$ Å). Residues are listed on the *X* axis as the concentration of position and chain list in the form of chain/triplet number (example: A3 is the third triplet in chain A). From left to right the residues shown are A1, B1, C1, A2, B2, C2, . . . A30, B30, C30. Five different substituted prolines in the Y position are shown. PPG is $[(\text{Pro–Pro–Gly})_{10}]_3$. PHG is $[(\text{Pro–Hyp–Gly})_{10}]_3$. PFG is $[(\text{Pro–Flp–Gly})_{10}]_3$. PNG is $[(\text{Pro–Amp–Gly})_{10}]_3$. PMG is $[(\text{Pro–Amp}^{1+}\text{–Gly})_{10}]_3$ The figure shows repeated differences in solvent number depending on the residue type, illustrating that different triplets likely affect solvent structure.

nine substitutions destabilize the triple helix.[26] Other employing molecular mechanics with implicit solvation models (mm/PBSA)[27] may be helpful in building new energetic models for collagen and describing the components that lead to Cγ-*exo* stabilization.

It is with great sadness that we acknowledge the death of our colleague, mentor and friend, Professor Peter Andrew Kollman after a brief bout with cancer. He will be mourned by the scientific community at large. The authors would also like to acknowledge Jun Mei Wang for help with the Antechamber component of AMBER, Giselle Knudsen for Figure 1 and the NIH Research Resource for Biomolecular Graphics at UCSF for use of their facilities. This work is funded by NIH grant AR47720-01 (T. Klein, PI).

REFERENCES

1. Kersteen, E.; Raines, R. Biopolymers 2001, 59, 24–28.
2. Berg, R.; Prockop, D. Biochem Biophys Res Commun 1973, 52(1), 115–120.
3. Holmgren, S.; Bretscher, L.; Taylor, K.; Raines, R. Chem Biol 1999, 6(2), 63–70.
4. Sakakiba, S.; Inouye, K.; Shudo, K.; Kishida, Y.; Kobayash, Y.; Prockop, D. Biochim Biophys Acta 1973, 303(1), 198–202.
5. Ramachandran, G.; Bansal, M.; Bhatnagar, R. Biochem Biophys Acta 1973, 322(1), 166–171.
6. Okuyama, K.; Arnott, S.; Takayangi, M.; Kakudo, M. J Mol Biol 1981, 152(2), 427–443.
7. Migchels, C.; Berendse, H. J Chem Phys 1973, 59(1), 296–305.
8. Holmgren, S.; Taylor, K.; Bretscher, L.; Raines, R. Nature 1998, 392, 666–667.
9. Babu, I.; Ganesh, K. J Am Chem Soc 2001, 123(9), 2079–2080.
10. Bretscher, L.; Jenkins, C.; Taylor, K.; DeRider, M.; Raines, R. J Am Chem Soc 2001, 123(4), 777–778.
11. Inouye, K.; Sakakibara, S.; Prockop, D. Biochim Biophys Acta 1976, 420(1), 133–141.
12. Inouye, K.; Kobayashi, Y.; Kyogoku, Y.; Kishida, Y.; Sakakibara, S.; Prockop, D. Arch Biochem Biophys 1982, 219(1), 198–203.

13. Panasik, N.; Eberhardt, E.; Edison, A.; Powell, D.; Raines, R. Int J Peptide Protein Res 1994, 44(3), 262–269.
14. O'Hagan, D.; Bilton, C.; Howard, J.; Knight, L.; Tozer, D. J Chem Soc Perkin Trans 2 2000, 4, 605–607.
15. Vitagliano, L.; Berisio, R.; Mazzarella, L.; Zagari, A. Biopolymers 2001, 58, 459–464.
16. Howard, A.; Cieplak, P.; Kollman, P. J Comput Chem 1995, 16(2), 243–261.
17. Klein, T.; Huang, C. Biopolymers 1999, 49(2), 167–183.
18. Bayly, C.; Cieplak, P.; Cornell, W.; Kollman, P. J Phys Chem 1993, 97(40), 10269–10280.
19. Cieplak, P.; Cornell, W.; Bayly, C.; Kollman, P. J Comput Chem 1995, 16(11), 1357–1377.
20. Macarthur, M.; Thornton, J. J Mol Biol 1991, 218(2), 397–412.
21. Frisch, M. J.; Trucks, G. W.; Schlegel, H. B.; Scuseria, G. E.; Robb, M. A.; Cheeseman, J. R.; Zakrzewski, V. G.; Montgomery, J. A.; Stratmann, R. E.; Burant, J. C.; Dapprich, S.; Millam, J. M.; Daniels, A. D.; Kudin, K. N.; Strain, M. C.; Farkas, O.; Tomasi, J.; Barone, V.; Cossi, M.; Cammi, R.; Mennucci, B.; Pomelli, C.; Adamo, C.; Clifford, S.; Ochterski, J.; Petersson, G. A.; Ayala, P. Y.; Cui, Q.; Morokuma, K.; Malick, D. K.; Rabuck, A. D.; Raghavachari, K.; Foresman, J. B.; Cioslowski, J.; Ortiz, J. V.; Stefanov, B. B.; Liu, G.; Liashenko, A.; Piskorz, P.; Komaromi, I.; Gomperts, R.; Martin, R. L.; Fox, D. J.; Keith, T.; Al-Laham, M. A.; Peng, C. Y.; Nanayakkara, A.; Gonzalez, C.; Challacombe, M.; Gill, P. M. W.; Johnson, B. G.; Chen, W.; Wong, M. W. Andres, J. L.; Head-Gordon, M.; Replogle, E. S.; Pople, J. A. Gaussian 98 (Revision A.7); Gaussian: Pittsburgh, PA, 1998.
22. Bella, J.; Eaton, M.; Brodsky, B.; Berman, H. Science 1994, 266, 5182.
23. Kramer, R.; Vitagliano, L.; Bella, J.; Berisio, R.; Mazzarella, L.; Brodsky, B.; Zagari, A.; Berman, H. J Mol Biol 1998, 280(4), 623–638.
24. Li, M.; Fan, P.; Brodsky, B.; Baum, J. Biochemistry 1993, 32(48), 13299–13309.
25. Bella, J.; Brodsky, B.; Berman, H. Connective Tissue Res 1996, 35(1–4), 401–406[455–460].
26. Mooney, S.; C.; Huang, P.; Kollman, and T.; Klein, Biopolymers 2001, 58(3) ,347–353.
27. Kollman, P.; Massova, I.; Reyes, C.; Kuhn, B.; Huo, S.; Chong, L.; Lee, M.; Duan, Y.; Wang, W.; Donini, O.; Cieplak, P.; Srinivasan, J.; Case, D.; Cheatham, T. Acc Chem Res 2000, 33(12), 889–897.
28. Fraser, R.; MacRae, T.; Suzuki, E. J Mol Biol 1979, 129, 463–481.